Optics Communications xxx (2008) xxx–xxx

Contents lists available at ScienceDirect

Optics Communications

journal homepage: www.elsevier.com/locate/optcom

Thermal effects investigation and cavity design in passively mode-locked Nd:YVO_4 laser with a SESAM

Tao Li [a], Shengzhi Zhao [a,*], Zhuang Zhuo [a], Yonggang Wang [b]

[a] School of Information Science and Engineering, Shandong University, Jinan, Shandong 250100, China
[b] Institute of Semiconductors, The Chinese Academy of Sciences, Beijing 100083, China

ARTICLE INFO

Article history:
Received 19 September 2008
Received in revised form 29 October 2008
Accepted 3 November 2008
Available online xxxx

PACS:
42.55.Xi
42.55.Rz
42.70.Hj
42.60.Da

Keywords:
Nd:YVO_4 crystal
SESAM
Mode-locking
Thermal effects

ABSTRACT

A diode-pumped passively mode-locked Nd:YVO_4 laser with a five-mirror folded cavity is presented by using a semiconductor saturable absorber mirror (SESAM). The temperature distribution and thermal lensing in laser medium are numerically analyzed to design a special cavity which can keep the power density on SESAM under its damage threshold. Both the Q-switched and continuous-wave mode-locked operation are experimentally realized. The maximum average output power of 8.94 W with a 9.3 ps pulse width at a repetition rate of 111 MHz is obtained under a pump power of 24 W, correspondingly the optical slope efficiency is 39.2%.

1. Introduction

Laser material Nd:YVO_4, due to its high absorption coefficient and large stimulated emission cross section, is considered to be suitable for constructing diode-pumped picoseconds laser [1–7]. However, the weak thermal conduction limits its application in high-power, ultra-short-pulse mode-locked laser systems [8–10]. Refs. [5,11] have reported 6.2 W and 8.1 W averaged output power with the conversion efficiency of 35% and 41% by adopting the SESAMs respectively, but both mode-locked lasers are demonstrated with Z cavity and the output is separated into two-beams, which are not convenient for practical applications.

The main obstacles for high average output power mode-locked laser are the thermal effect and SESAM's damage. It is valuable to analyze the thermal lens in Nd:YVO_4 crystal, which affects the output power of the laser and the stability of the resonator. In this paper, by adopting a finite element method to simulate the temperature distribution in Nd:YVO_4 crystal, we obtain the thermal focal length of laser medium. Based on the theoretical calculations, a five-mirror cavity is designed masterly to keep the power density on SESAM under its damage threshold and simultaneously has a good mode matching in the laser crystal. Finally, a CW mode-locked laser with the pulse width of 9.3 ps has been realized successfully at a repetition rate of 111 MHz. The output mode-locked laser has only one beam, and reaches an average power of 8.94 W with the peak power of 8.6 kW.

2. Theoretical simulation of the thermal lens

The thermal distortions in laser rods have been widely investigated. Innocenzi et al. [12] gave the focal length of the thermal lens as

$$f_T = \frac{2\pi K_c \omega_p^2}{P_T(dn/dT)} \frac{1}{1-\exp(-\alpha l)} \tag{1}$$

where P_T is fraction of pump power that results in heating, ω_P is the radius of the pump beam, K_c is the thermal conductivity, dn/dT is the thermal dispersion coefficient, α is the absorber coefficient, l is the crystal length.

Eq. (1) is used frequently in resonator design [13–15]. However, it is only applicable for isotropic rod laser crystal, and it just considers the contribution of thermal dispersion while neglecting the influence from the end face curvature [15]. In order to simulate

* Corresponding author.
E-mail address: shengzhi_zhao@sdu.edu.cn (S. Zhao).

0030-4018/$ - see front matter © 2008 Elsevier B.V. All rights reserved.
doi:10.1016/j.optcom.2008.11.008

the thermal effects of $Nd:YVO_4$ crystal more accurately, we adopt the finite element method and consider its anisotropic thermal conductivity.

The a-cut $Nd:YVO_4$ crystal used in this experiment has a dimensions of $a \times b \times l = 4 \times 4 \times 7\ \mathrm{mm}^3$. One end facet of the crystal is coated antireflection (AR) at 808 nm and high reflection (HR) at 1064 nm, while the other end facet is AR coated at 1064 nm. The $Nd:YVO_4$ crystal is wrapped with indium foil and fitted into a copper housing which is cooled by water at a constant temperature of 289 K. In this case, the temperature profile in laser crystal is expressed by the three dimensional Poisson equation as

$$K_x \frac{\partial^2 T(x,y,z)}{\partial x^2} + K_y \frac{\partial^2 T(x,y,z)}{\partial y^2} + K_z \frac{\partial^2 T(x,y,z)}{\partial z^2} + q(x,y,z) = 0 \qquad (2)$$

where x, y are the transverse coordinates, z is the longitudinal coordinate with the value of $z = 0$ at the pumped end of the crystal; K_x, K_y, and K_z are the heat conductivity coefficients of axis x, y, and z, respectively; T is the temperature. The thermal density $q(x,y,z)$ along the resonator axis in the crystal can be expressed as Gaussian function [15]

$$q(x,y,z) = \frac{2Q\alpha}{\pi\omega_p^2(z)}(1 - e^{-\alpha l})e^{-2\left[\left(x-\frac{a}{2}\right)^2+\left(y-\frac{b}{2}\right)^2\right]/\omega_p^2(z)}e^{-\alpha z} \qquad (3)$$

where Q is the total heat load, and in $Nd:YVO_4$ the quantum defect is a fraction 0.24 of the absorbed pump power. On the basis of paraxial approximation, the radius of the pump light in laser crystal may be given by

$$\omega_P(z) = \omega_{P0} + \theta_P|z - z_0| \qquad (4)$$

where ω_{P0} is the radius at the pump beam waist; θ_P is the far-filed half-angle and z_0 is the distance between the focal plane of pump beam and the pumped facet of laser medium.

The thermal conductivity of heat sink is much greater than that of laser crystal. The temperature at the surrounding surfaces of laser crystal is supposed to be the same as water temperature. The boundary conditions can be expressed as

$$T\left(-\frac{a}{2},y,z\right) = 289; \qquad T\left(\frac{a}{2},y,z\right) = 289 \qquad (5)$$

$$T\left(-\frac{b}{2},y,z\right) = 289; \qquad T\left(\frac{b}{2},y,z\right) = 289 \qquad (6)$$

$$\frac{\partial T(x,y,z)}{\partial z}\Big|_{z=0} = h(T - T_{\mathrm{air}}); \frac{\partial T(x,y,z)}{\partial z}\Big|_{z=l} = -h(T - T_{\mathrm{air}}) \qquad (7)$$

Here h is heat transfer coefficient between the laser crystal surface and air; T_{air} s the room temperature with a value of 300 K.

According to the corresponding parameters shown in Table 1, by numerically solving coupled Eqs. (2)–(7), we obtain the temperature rise in laser crystal. Fig. 1 shows a two-dimensional (cross x–y section) temperature distribution. At the pump power of 25 W, the highest temperature in the center of the pumped facet is 585.8 K, resulting in a temperature rising of 296.8 K.

The inhomogeneous temperature distribution in crystal results in the changes of refractive index. For light propagating along the resonator axis, the beam distortion and wavefront variation are

Table 1
Parameters used in the simulation.

Parameters	Values	Parameters	Values
K_x	$5.1\ \mathrm{Wm^{-1}\,K^{-1}}$	n_0	2.183
K_y	$5.23\ \mathrm{Wm^{-1}\,K^{-1}}$	α_z	$4.43 \times 10^{-6}\ \mathrm{K^{-1}}$
K_z	$5.1\ \mathrm{Wm^{-1}\,K^{-1}}$	$\partial n/\partial T$	$8.5 \times 10^{-6}\ \mathrm{K^{-1}}$
ω_{P0}	320 μm	T_0	289 K
α	$5.32\ \mathrm{cm^{-1}}$	h	$4\ \mathrm{Wm^{-2}\,K^{-1}}$
θ_P	1.5 mrad	z_0	1 mm

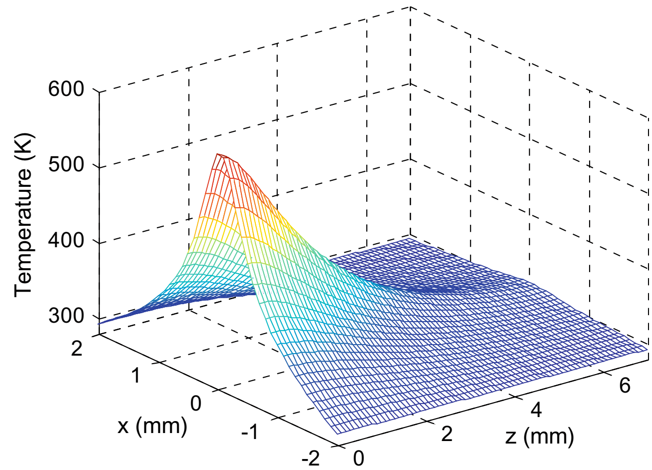

Fig. 1. The temperature distribution in x–z section ($y = 0$) at pump power of 25 W.

appearing. The optical path difference (OPD) for one pass through the crystal can be written as [16]

$$\mathrm{OPD}(x,y) = n_0\alpha_z \int_0^l [T(x,y,z) - T_0]dz + \int_0^l \frac{\partial n}{\partial T} T(x,y)dz \qquad (8)$$

where n nd n_0 are the refractive index of the crystal at the temperature T and the room temperature, respectively, α_z s the thermal expansion coefficient, T_0 is the initial temperature. In the pumped region, it is common to consider the laser crystal to be a thermally induced spherical convex lens. The focal length of the lens could be derived from the Eq. (8)

$$f(x,y) = (x^2 + y^2)/2(\mathrm{OPD}_o - \mathrm{OPD}(x,y)) \qquad (9)$$

where OPD_0 denotes the OPD in the center.

Fig. 2 Shows the focal length of the thermally induced lens as a function of the pump power, which is numerically obtained and compared with the value of Eq. (1).

For the experimental configuration which is shown in Fig. 5, using the well-known ABCD matrix method and considering the thermal lens effect of the laser medium, we have simulated the radii of the TEM_{00} mode as shown in Fig. 3. With the increase of pump power, the variations of TEM_{00} mode radii are about 300–400 μm in the laser crystal and 30–80 μm on the SESAM, respectively. From Fig. 3, it can be also seen that TEM_{00} mode radii on the SESAM increases with the pump power, preventing the SESAM from damage under high pump power.

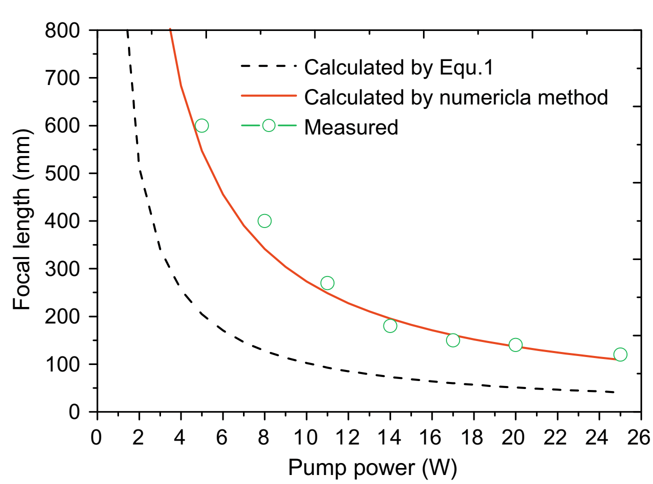

Fig. 2. The focal length of thermal lens versus pump power.

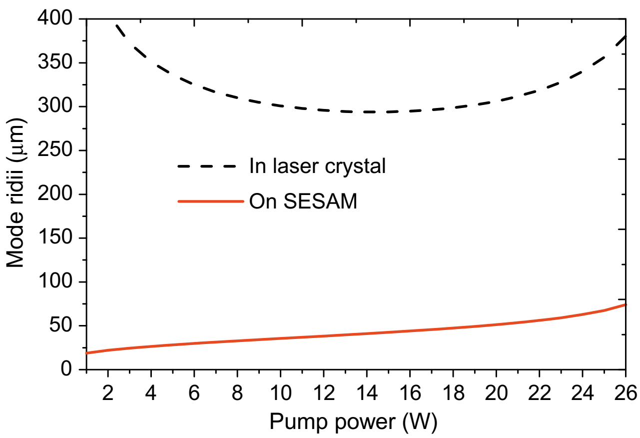

Fig. 3. The dependence of beam size on pump power.

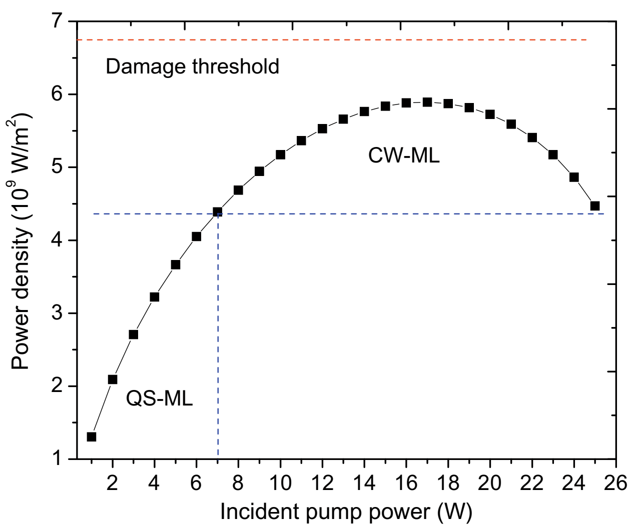

Fig. 4. Power density on SESAM versus incident pump power.

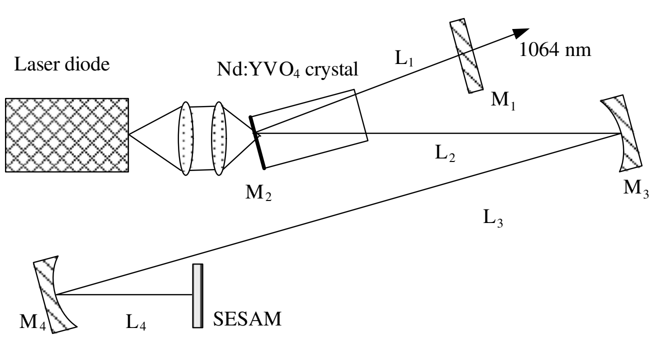

Fig. 5. Cavity configuration of the passively mode-locked Nd:YVO_4 laser.

The power density on SESAM can be expressed as

$$\rho = P_{\rm in}\eta\pi^{-1}\omega_s^{-2}\frac{1+R}{1-R} \tag{10}$$

where $P_{\rm in}$ is the incident pump power, η is the transfer efficiency of the pump power to the output power, ω_s is the radii of TEM_{00} mode on SESAM and R is the reflection of the output coupler. In order to determine the SESAM's damage threshold, we use a flat mirror with reflection of 90% instead of M_1. When the pump power is increased to 15 W, the output power decreases abruptly which indicates the

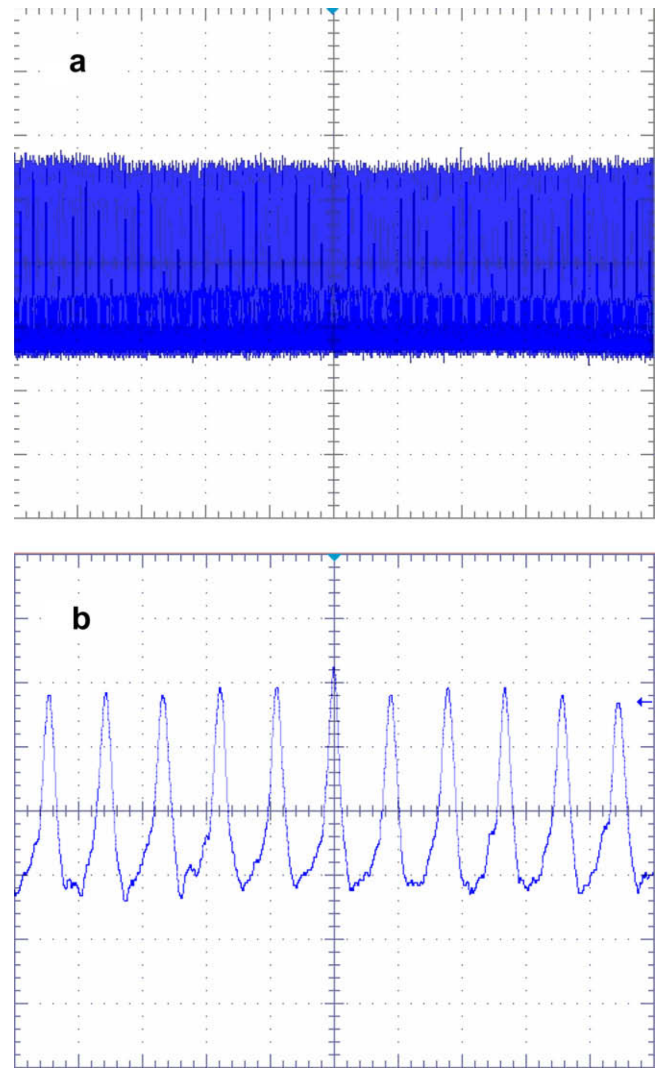

Fig. 6. Pulse train of the CW mode-locked Nd:YVO_4 laser with time delay of (a) 1 μs an (b)10 ns, respectively.

SESAM have been destroyed. A maximum output power of 1.5 W is obtained. Accordingly, the damage threshold can be approximately calculated from the Eq. (9) to be 0.678 MW/cm^2. In our mode-locked laser, the reflection of M_1 is 80% and the output power increases with pump power at an almost linear proportion with a value of 37.3% (as shown in Fig. 7). By taking those parameters into the Eq. (9) we can obtain the relationship between the power density on SESAM and the incident pump power which has been shown in Fig. 4. Apparently, the power density is lower than SESAM's damage threshold meanwhile exceeding the Q-switched mode-locking threshold during the pump range from 7 W to 25 W, which indicate a reasonable cavity design.

3. Experimental setup

Based on the thermal effect analysis, a five-mirrors folded cavity is adopted in this experiment to realize the mode-locked Nd:YVO_4 laser. A schematic of the laser configuration is shown in Fig. 5. A flat mirror M_1 with a reflection of 20%, acting as the output coupler, is positioned 100 mm away from laser crystal, M_2 coated on YVO_4 crystal acts as one resonator mirror. M_3 and M_4 are HR at 1064 nm with radii of curvature of 500 mm and 200 mm, respectively. The Nd:YVO_4 crystal is pumped by a fiber coupled diode laser with

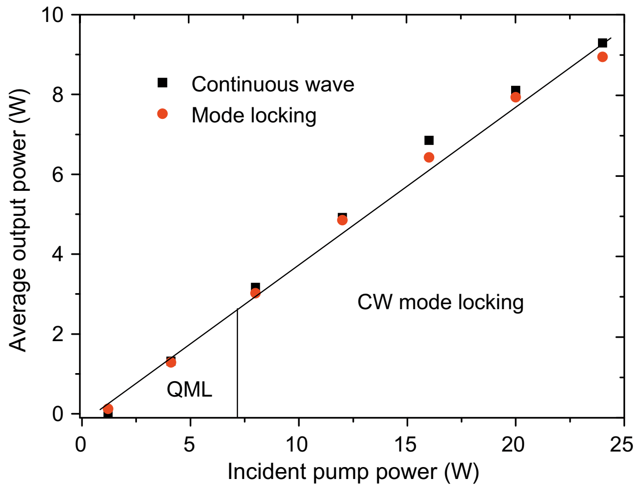

Fig. 7. Average output power versus the pump power.

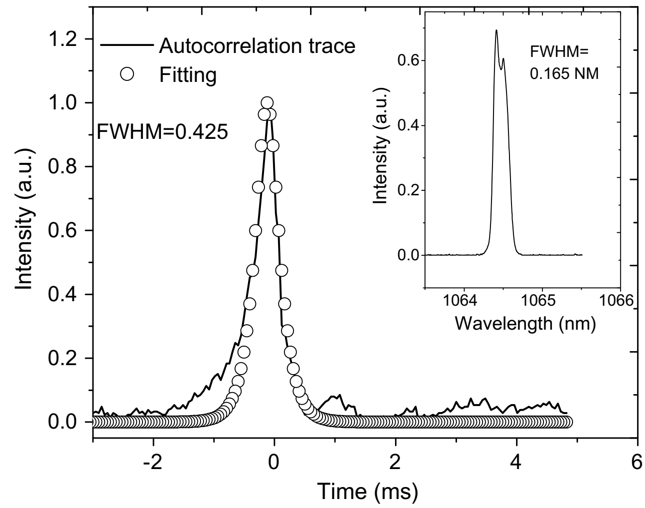

Fig. 8. Autocorrelation trace of the output pulses. Solid line: autocorrelation signal of CW mode-locked pulses; circle line: Gaussian fitting and insert: output spectrum.

the wavelength of 808 nm at 25 °C. The cavity parameters are rationally optimized in principle to generate a reasonable focused beam on the SESAM and have a good mode matching in the laser crystal. The total cavity length is about 135.5 cm.

4. Results and discussion

A Q-switched mode-locked state is initiated with the pump power from 1.2 W to 7 W. The picoseconds pulses are superimposed upon the long Q-switched envelope with a full width at half-maximum of about 200 ns and a repetition rate of 69–285 kHz. When the pump power rises above 7 W, the laser will show typical CW mode-locking operation with a repetition rate of 111 MHz as determined by the cavity length. Fig. 6a,b shows the CW mode-locked pulse train on a different time scale, detected by a Tektronics oscilloscope (Tek.TDS 5104) via a fast response photo-detector.

The average output power versus incident pump power is shown by scattered dots in Fig. 7. The laser threshold is 1.2 W and the maximum average output power is about 8.94 W at the pump power of 24 W, corresponding to an optical slope efficiency of 39.2%. In comparison with CW operation, the output power of CW mode-locked laser is only slightly decreased and the SESAM is not damaged during the operation. The fluctuation $\Delta\bar{P}$ of output power is tested at 15 W pump power, with a time interval of 5 min. If $\Delta\bar{P}$ is given by $\Delta\bar{P} = [\sum_{i-1}^{n}(P_i - \bar{P})^2/n]^{1/2}$, the instability $\Delta\bar{P}/\bar{P}$ of the laser is 0.19%.

The mode-locked pulse width is measured with an autocorrelator (FR-103XL, Femtochrome Research Inc). Fig. 8 shows the oscilloscope trace of a CW mode-locked pulse train. The full width at half maximum (FWHM) trace width is around 425 µs, correspondingly the pulse duration is fitted to be 9.3 ps. The pulse peak power is thus calculated to be 8.7 kW for the average output power of 8.94 W. The CW mode-locked laser spectrum is also measured by using an optical spectrum analyzer (ANDO AQ-6315 A) as shown in Fig. 8 (inset). It is found that the laser oscillates at around 1064.5 nm and the bandwidth of the laser spectrum is about 0.165 nm, corresponding to $\Delta v = 43.7$ GHz, which could support pulses of 9.3 ps duration. The time-bandwidth product is $\Delta v \Delta t = 0.41$.

5. Conclusion

In summary, we have successfully demonstrated a passively mode-locked $Nd{:}YVO_4$ laser with a SESAM. By using a five-mirror fold cavity, the mode-locked output power of 8.94 W is obtained with a repetition rate of 111 MHz at the incident pump power of 24 W. The instability $\Delta\bar{P}/\bar{P}$ of the lasers is 0.19% at the pump power of 15 W. No damage to the SESAM is observed during the laser operation, which indicates a reasonable cavity design with the theoretical simulation of the thermal lens.

Acknowledgments

This work was partially supported by the National Science Foundation of China (60578010) and the Natural Science Foundation of Shandong Province (Y2005G10).

References

[1] R. Fluck, B. Braun, E. Gini, H. Melchior, U. Keller, Opt. Lett. 22 (1997) 991.
[2] L. Krainer, R. Paschotta, J. Ausder, C. Honninger, U. Keller, M. Moser, D. Kopf, K.J. Weigarten, Appl. Phys. B. 69 (1999) 245.
[3] Y.F. Chen, S.W. Tsai, C. Wang, F. Huang, Opt. Lett. 26 (2001) 199.
[4] R. Fluck, G. Zhang, U. Keller, K.J. Weingarten, M. Moser, Opt. Lett. 21 (1996) 1378.
[5] Zhiqiang Cai, Wu-qi Wen, Jian-quan Yao, Yong-gang Wang, Zhi-gang Zhang, Jian-yong Zhou, Jia-ning Zhou, Peng Wang, Chin. Opt. Lett. 3 (2005) 342.
[6] Y.F. Chen, S.W. Tsai, IEEE J. Quantum Electron. 37 (2001) 580.
[7] P.K. Mukhopadhyaya, M.B. Alsousb, K. Ranganathana, S.K. Sharmaa, P.K. Guptac, J. Georgea, T.P.S. Nathana, Opt. Commun. 222 (2003) 399.
[8] Feng Song, Chaobo Zhang, Xin Ding, Jingjun Xu, Guangyin Zhang, Matthew Leigh, Nasser Peyghambarian, Appl. Phys. Lett. 81 (2002) 2145.
[9] Akira Sugiyama, Yasunaga Nara, Ceram. Int. 31 (2005) 1085.
[10] Z. Ma, D. Li, J. Gao, N. Wu, K. Du, Opt. Commun. 275 (2007) 179.
[11] J.Y. Peng, J.G. Miao, Y.G. Wang, B.S. Wang, H.M. Tan, L.S. Qian, X.Y. Ma, Opt. Laser Technol. 39 (2007) 1135.
[12] M. Innocenzi, H. Yura, C. Fincher, R. Fieids, Appl. Phys. Lett. 56 (1990) 1831.
[13] K.J. Yang, S.Z. Zhao, G.Q. Li, H.M. Zhao, IEEE J. Quantum Electron. 40 (2004) 1252.
[14] F. Song, C.B. Zhang, X. Ding, J.J. Xu, G.Y. Zhang, M. Leigh, N. Peyghambarian, Appl. Phys. Lett. 81 (2002) 2145.
[15] Y.F. Chen, T.M. Huang, C.F. Kao, C.L. Wang, S.C. Wang, IEEE J. Quantum Electron. 33 (1997) 1424.
[16] C. Pfistner, R. Weber, H.P. Weber, S. Merazzi, R. Gruber, IEEE J. Quantum Electron. 30 (1994) 1605.